Ferroelectric state analysis in grain boundary of Na 0.85 Li 0.15 NbO 3 ceramic

M. A. L. Nobre and S. Lanfredi

Citation: Journal of Applied Physics **93**, 5557 (2003); doi: 10.1063/1.1564281
View online: http://dx.doi.org/10.1063/1.1564281
View Table of Contents: http://scitation.aip.org/content/aip/journal/jap/93/9?ver=pdfcov
Published by the AIP Publishing

Ferroelectric state analysis in grain boundary of $Na_{0.85}Li_{0.15}NbO_3$ ceramic

M. A. L. Nobre[a] and S. Lanfredi[a),b)]
Faculdade de Ciências e Tecnologia-FCT, Universidade Estadual Paulista-UNESP, Caixa Postal 467, 19060-900 Presidente Prudente, São Paulo, Brazil

(Received 22 October 2002; accepted 10 February 2003)

The electric and dielectric properties of the grain boundary of $Na_{0.85}Li_{0.15}NbO_3$ lead-free ferroelectric-semiconductor perovskite were investigated. The impedance spectroscopy was carried out as a function of a thermal cycle. The sodium lithium niobate was synthesized by a chemical route based on the evaporation method. Dense ceramic, relative density of 97%, was prepared at 1423 K for 2 h in air atmosphere. ac measurements were carried out in the frequency range of 5 Hz–13 MHz and from 673 to 1023 K. Theoretical adjust of the impedance data was performed to deriving the electric parameters of the grain boundary. The electric conductivity follows the Arrhenius law, with activation energy values equal to 1.55 and 1.54 eV for heating and cooling cycle, respectively. The nonferroelectric state of the grain boundary and its correlation with symmetry are discussed in the temperature domain. © *2003 American Institute of Physics.*
[DOI: 10.1063/1.1564281]

I. INTRODUCTION

$Na_{1-x}Li_xNbO_3$ solid solutions are a promising lead-free nonrelaxor ferroelectric material.[1] $NaNbO_3$ host structure has been found to be ferroelectric at room temperature for doping with lithium fractions of $x \geqslant 0.015$.[1,2] Thus, the addition of cations lithium, even in small amounts, leads to development of a ferroelectric state, which makes $Na_{1-x}Li_xNbO_3$ ceramic system a suitable for high temperature and frequency applications involving piezoelectric, pyroelectric, electro-optic, and ferroelastic properties. Reports on the optical studies in $Na_{0.98}Li_{0.02}NbO_3$ single crystal have described five phase transitions between 163 and 940 K, with the Curie temperature found at around 640 K.[3] Considering $Na_{1-x}Li_xNbO_3$ systems, the increase of substitution level of Na^+ by Li^+ in $Na_{1-x}Li_xNbO_3$ system increases Curie's temperature. Several investigations have been performed on the bulk properties of $Na_{1-x}Li_xNbO_3$ and $NaNbO_3$ being some of them recent.[4,5] However, no analysis has been addressed to the investigation of electric and dielectric phenomena of the grain boundary of this system. A series of difficulties involves the characterization of properties of the grain boundary. Some of them are related to ceramic microstructure, in which the proper development is affected by powder preparation method and sintering parameters.

Polycrystalline sodium lithium niobate has traditionally been prepared by conventional way based on the mechanical mixture of oxides and/or carbonates. This process involves several restrictions to powder features being all one inherent to this processing technique. As an example, metastables intermediate phases have been found, when $Na_{1-x}Li_xNbO_3$ powders are prepared by conventional methods.[6] Otherwise, chemical methods of oxide synthesis lead to simultaneous improvement of several chemistry and physic parameters such as stoichiometry, powder texture control, chemical homogeneity, and single phase.[7]

In general, few studies on the electrical and dielectrical behavior have been dedicated to polycrystalline $Na_{1-x}Li_xNbO_3$ systems synthesized via a chemical route, an enhanced powder. In this sense, the $Na_{0.85}Li_{0.15}NbO_3$ was synthesized by a chemical method through the thermal decomposition one of the precursor salt, which was prepared by the evaporation solution method.[8] This method gives rise a better control of the reagents, a low calcination temperature, a single phase material, and high specific surface area being suitable to attain ceramics with relative density very similar to the theoretical one.

In this article, a deep insight on the grain boundary properties in nonpoled $Na_{0.85}Li_{0.15}NbO_3$ ferroelectric dense ceramic is presented. The polarization phenomenon at grain boundary is discussed based on the relaxation characteristic.

II. EXPERIMENT

A. Synthesis

The synthesis of the $Na_{0.85}Li_{0.15}NbO_3$ precursor was performed by a chemical evaporation method, using a soluble niobium complex salt, $NH_4H_2[NbO(C_2O_4)_3]3H_2O$, provided by Companhia Brasileira de Metalurgia e Mineração, Araxá-MG, Brazil (CBMM), sodium nitrate and lithium nitrate as starting reagents. A saturated solution of oxalic acid was added to a 1 mol^{-1} solution of sodium nitrate and lithium nitrate in deionized water. The *p*H of the solution was monitored by a digital *p*H meter, until a value equal to 1 was reached. Then, the *p*H was raised to 3 by addition of a 1:1 ammonium hydroxide solution. After the stirring for 10 min, a 0.7 $mol\,l^{-1}$ niobium salt solution was added, leading to a final solution of *p*H equal to 2. In the sequence, this

a)Member of the UNESP/CVMat-Virtual Center of Research in Materials.
b)Author to whom correspondence should be addressed; electronic mail: silvania@prudente.unesp.br

solution was refluxed for 3 h at 353 K. After refluxing, the solution was maintained at 343 K until the point of complete water evaporation and formation of a solid material. The one was deagglomerated in an agate mortar being termed of precursor, which was spread in an alumina substrate and calcined at several temperatures between 523 and 973 K during 5 h. Crystalline powder of $NaNbO_3$ single phase (JCPDS card number 33-1270)[9] was prepared by calcination of the precursor powder at 973 K during 5 h, in air atmosphere.

B. Compaction and sintering

$Na_{0.85}Li_{0.15}NbO_3$ green compact was prepared by uniaxial pressing at 10 kPa and subsequent isostatic pressing at 100 MPa. The sintering process was performed in a box furnace air atmosphere, under dry air flux, at 1423 K during 2 h. A 283 K/min heating rate was employed, while the cooling rate was fixed the thermal inertia of the furnace. A relative density of 97% of the theoretical one was reached.

C. Complex impedance characterization

All measurements were carried out by impedance spectroscopy. The one were performed in the frequency range of 5 Hz–13 MHz, using a Hewlett-Packard HP 4192A impedance analyzer controlled by a personal computer. Platinum electrodes were deposited on both faces of the sample by a platinum paste coating (Demetron 308A), which was dried at 1073 K for 30 min. The nominal applied voltage was 500 mV. A sample holder with a two-electrode configuration was used. The ac measurements were taken from 673–1023 K in 323 K temperature steps. The temperature was kept stable for 1 h prior to each measurement. The heating or cooling rate was equal to 278 K/min. All the measurements were carried out in static air atmosphere. The impedance data, $Z^*(\omega)$, were normalized by reciprocal geometric factor S/l, where S is the electrode area and l is the thickness of the sample. Theoretical adjust of the impedance data were realized using a specific software,[10] which allows to determine of electric parameters such as resistance and capacitance with a precision better than 3%.

III. RESULTS AND DISCUSSIONS

A. Conductivity analysis

Figures 1(a)–1(b) shows the impedance diagrams of the $Na_{0.85}Li_{0.15}NbO_3$ ceramic obtained at 773 and 823 K, in the heating and cooling cycles. A thermal hysteresis development can be identified during heating-cooling cycle at all temperatures investigated. Furthermore, the hysteresis phenomenon occurs with the increase of the resistivity during the cooling cycle. The impedance diagrams show a typical semicircle response at temperatures above 673 K. All semicircles are slightly depressed instead of centered on the abscissa axis. The most accepted approach to interpret the semicircle depression phenomenon is to consider them as being due a statistical distributions of relaxation times.[11] In an opposite sense, according to Debye's model, a material having a single relaxation time gives rise an ideal semicircle centered on the abscissa axis. The diagrams shape suggests

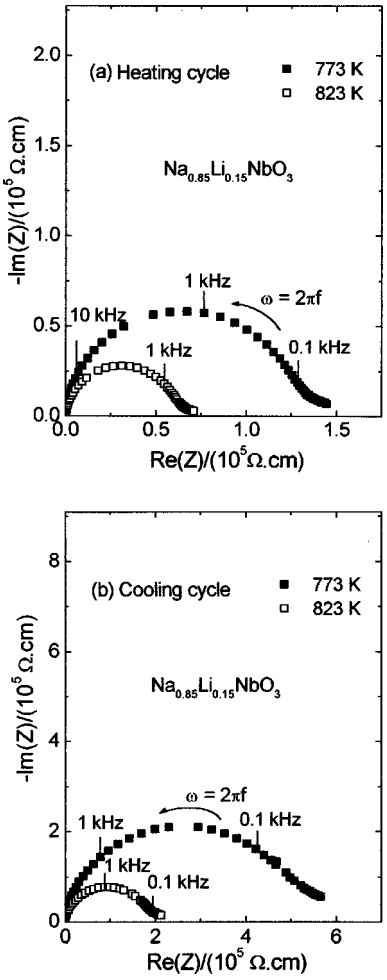

FIG. 1. Impedance diagrams of the $Na_{0.85}Li_{0.15}NbO_3$ polycrystal obtained at 773 and 823 K in one thermal cycle: (a) heating and (b) cooling.

that the electrical response is composed of at least two phenomena of relaxation with different relaxation frequencies. Furthermore, both relaxation phenomena obey a non-Debye model. This is further evidence that both the contributions follow a Cole–Cole type model.[12] Based on the previous assumptions, the response, $Z^*(\omega)$, has been assigned to grain and grain boundary one.[11] Then, the total impedance is described by relation $Z^*(\omega)=Z_g^*(\omega)+Z_{gb}^*(\omega)$ being the subscripts ascribed to the grain (g) and grain boundary (gb), respectively. These contributions can be simultaneously derived from theoretical adjust of the experimental data. In fact, this means that the electric parameters of both grain and grain boundary regions are extract.

An equivalent electric circuit and its respective resistance and capacitance components were derived for $Na_{0.85}Li_{0.15}NbO_3$ ceramic, as shown in Fig. 2. The points on the plot represent the experimental data, while the continuous line represents the theoretical adjust. The complex impedance characterization of the solid solution are well represented by two parallel RC equivalent circuits in series, see inset in Fig. 2.

An excellent agreement between the experimental points and the theoretical curve was obtained for all diagrams. The first semicircle positioned in the high frequency range

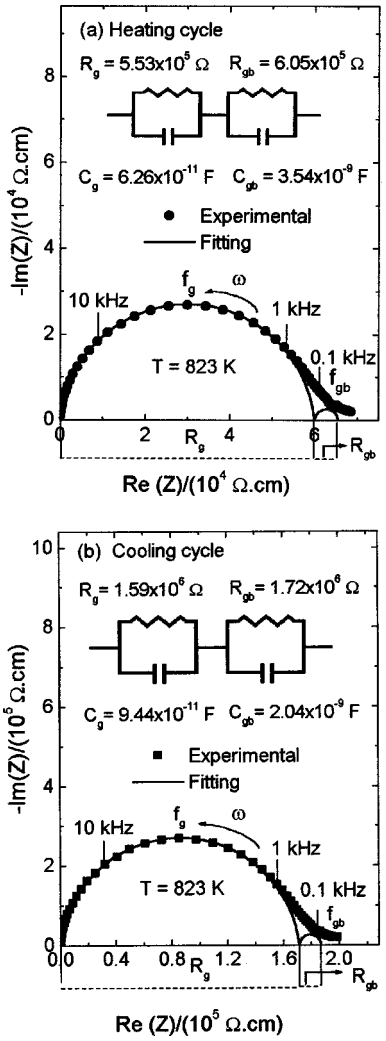

FIG. 2. Impedance diagrams of the $Na_{0.85}Li_{0.15}NbO_3$ polycrystal at 823 K. Two parallel *RC* equivalent circuits are shown in the inset, corresponding to the grain and grain boundary response of the solid solution in one thermal cycle: (a) heating and (b) cooling.

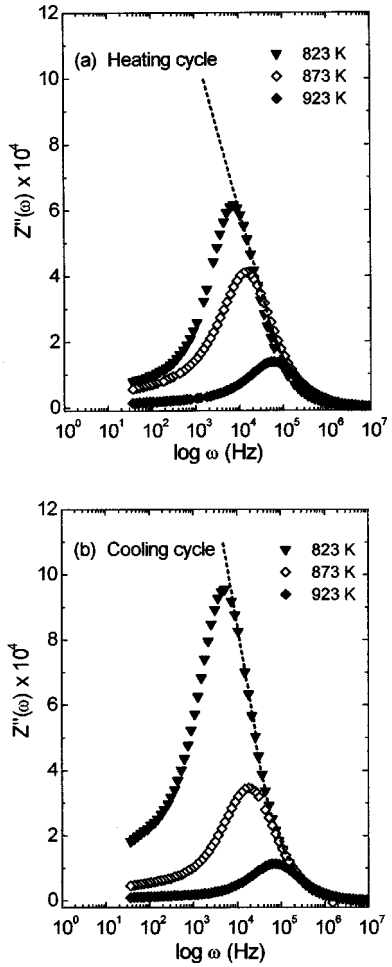

FIG. 3. Imaginary part of impedance Z'' as a function of frequency at several temperatures obtained in one thermal cycle: (a) heating and (b) cooling.

($>10^2$ Hz) stems from bulk properties. The second one ranging at low frequency values ($<10^2$ Hz) represents the grain boundary contribution.

Figures 3(a) and 3(b) shows imaginary part of impedance, $Z''(\omega)$, as a function of frequency at several temperatures during heating and cooling cycles, respectively. The curves show broad and asymmetric peaks at around a maximum in frequency suggesting a distribution of relaxation times. Moreover, the frequency of the maximum, an apparent relaxation frequency, shifts to more high values with increasing of the temperature. This behavior has been reported for several single crystals[13,14] being evidence of actuation of a hopping type mechanism as small polaron hopping with gradual decrease of electron-lattice coupling.

The electric resistance of $Na_{0.85}Li_{0.15}NbO_3$ grain boundary as a function of the reciprocal temperature was plotted as $\log(R_{gb})$ vs $10^3/T$. The resistance follows Arrhenius' law, given by the following equation:

$$R_{gb} = R_0 \exp(-E_a/kT), \quad (1)$$

where R_0 represents the pre-exponential constant or characteristic resistance, k is the Boltzmann's constant, and E_a is the apparent activation energy for the conduction process.

Figures 4(a) and 4(b) shows Arrhenius' plot of grain boundary and grain resistance as a function of one thermal cycle, respectively. The evolution of the resistance depends on the heating and cooling cycles. Considering Fig. 4(a), the apparent activation energy for conduction process of grain boundary is equal to 1.55 and 1.54 eV, for heating and cooling cycle, respectively. These values are equals from experimental viewpoint. This indicates that the activation energy presents stable characteristics with relation to the thermal cycle; in opposite sense to the bulk one, see Fig. 4(b).

In addition, none anomaly on the grain-boundary resistance curve is observed at around 913 K, as can be observed in Fig. 4(b). Therefore, the homogeneous shift observed between both heating and cooling grain-resistance curves can be explained by existence of distinct pre-exponential constant (R_0), according to Eq. (1). These parameters, R_0, were derived by extrapolation measurements carried out during heating and cooling cycles. The values differ at around one order of magnitude. The evolution of resistances are described for heating and cooling cycles by the following equations:

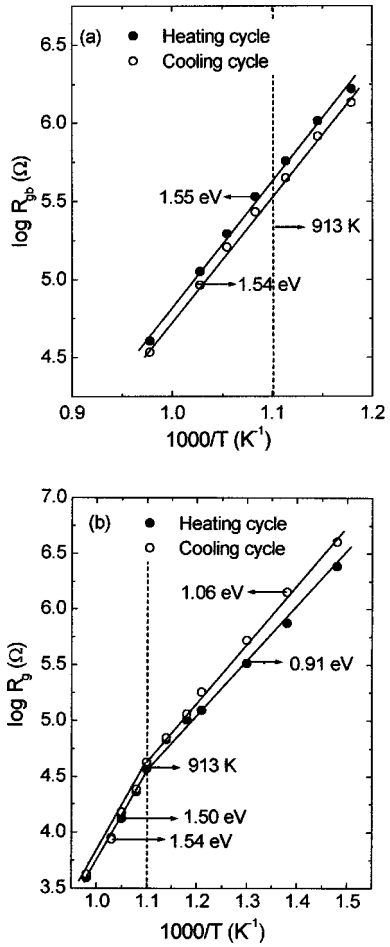

FIG. 4. Arrhenius diagram of resistance of the $Na_{0.85}Li_{0.15}NbO_3$ for one thermal cycle: (a) grain boundary and (b) grain.

$$R_{gb} = 1.98 \times 10^{26} \exp(-1.55/kT), \tag{2}$$

$$R_{gb} = 2.57 \times 10^{25} \exp(-1.54/kT). \tag{3}$$

As a whole, the grain boundary contributes to the electrical feature in a distinct way that the bulk contributes. As matter of fact, according to Fig. 4(b), both the characteristic resistance of the grain and activation energy values differ in a substantial manner depending on the temperature range of measurement and thermal cycle. Prior to gives sequence to data analysis and discussion, it is important to note that the activation energies derived at temperatures higher than 913 K are very similar to ones derived from Fig. 4(a). These values are derived for heating and cooling cycles being equals to 1.50 and 1.54 eV, respectively. This suggests strongly that a same conduction mechanism type is operational on the same or similar crystalline structures. As can be seem in Fig. 4(b), there is a clear resistance anomaly at around 913 K that leads to each branch of heating or cooling cycle to exhibit a distinct value of characteristic resistance and apparent activation energy of conduction process. This is in total accordance with previous work involving phase transitions analysis by dielectric spectroscopy.[15] In addition, the parameters R_0 were derived for bulk or grain differing in a significant manner of grain boundary one.

Taking into account previous discussion, a direct comparison between the grain boundary and grain resistance values is nontrivial, since the bulk presents a more complex temperature dependence of properties due phase transition phenomena.[15] At this point, considering the temperature range investigated, the existence of some kind of transition can be discarded. It seems that grain boundary no undergoes any structural phase transition.[15] Otherwise, we can hypothesize some indirect influence of bulk phase transition. However, a qualitative analysis of resistance values indicates that the resistance of the grain boundary differ until two orders of magnitude lower than of the grain, despite of similar activation energy. This changing would be compatible with the concept of grain boundary oxidation phenomenon. The Arrhenius diagram of the resistance of the grain of $Na_{0.85}Li_{0.15}NbO_3$, for a thermal cycle, exhibits two different regions clearly defined at temperature domain, in according to Fig. 4(b). Each branch has a distinct activation energy being both regions fairly susceptible to thermal cycles. Based on Fig. 4(b), the activation energy values of the grain are very similar to ones of the grain boundary at high temperature region (913 K) in accordance with Fig. 4(a). It is interesting to note that 913 K has been suggested as the temperature, in which occurs a pseudocubic or cubic distorted type to a cubic symmetry phase transition in the $NaNbO_3$ single crystals[3] and $Na_{0.85}Li_{0.15}NbO_3$ ceramic.[15] Thus, below 913 K, $NaNbO_3$ should exhibit structures with lower symmetry as orthorhombic, tetragonal or cubic distorted than above 913 K. The conduction mechanism of $Na_{1-x}Li_xNbO_3$ system is type small polaron, which is quite similar to $NaNbO_3$.[11,16] Considering the small polaron mechanism, the conductivity is a function of crystalline lattice polarization in the presence of electronic carriers, as well as carrier's number. For high temperature (>913 K), the quasi-independence of the activation energy with the thermal cycle and its magnitude indicates a low lattice polarization degree compatible with presence of only cubic or cubic distorted structure. Moreover, the temperature of 913 K is beyond of Curie's temperature, which is positioned at 708 K for $Na_{0.85}Li_{0.15}NbO_3$ ceramic.[15]

Based on the previous assumptions, we can assume that the grain boundary exhibits a cubic or cubic distorted structure, which should presents a almost linear dielectric character. In other words, according to the earlier assumptions, the grain boundary should exhibit a nonferroelectric character maintaining the poor-semiconductor character of bulk or grain (ferroelectric character).

B. Relaxation analysis

The grain boundary capacitance C_{gb} can be easily extracted, whether the complex plane representation is adopted. Then, the parameter C_{gb} is derived by the theoretical adjust of the experimental data, as shown in Fig. 2.

Figure 5 shows the reciprocal capacitance data of grain and grain boundary of $Na_{0.85}Li_{0.15}NbO_3$ as a function of temperature for the heating and cooling cycle. The grain boundary capacitance curve, $C_{gb} \times T$, shows a sharp evolution being almost independent of the temperature. Furthermore, the curve not present any evidence of phase transition in the

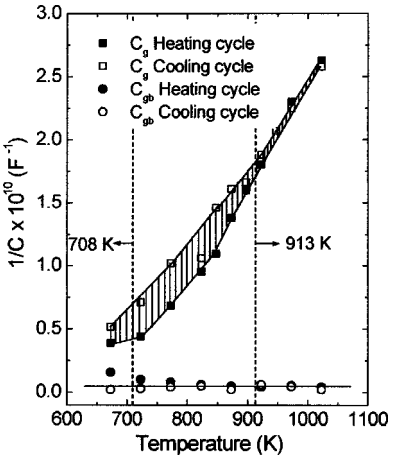

FIG. 5. Capacitance values of grain and grain boundary of the $Na_{0.85}Li_{0.15}NbO_3$ as a function of temperature in one thermal cycle.

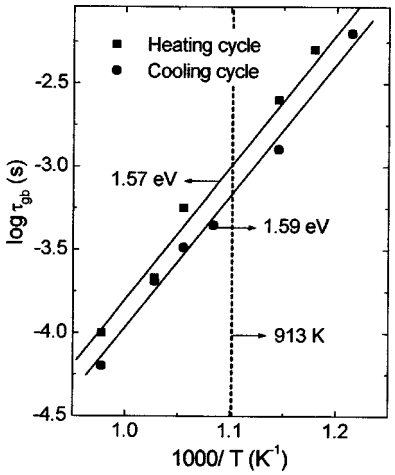

FIG. 6. Arrhenius diagram of grain boundary relaxation time of the $Na_{0.85}Li_{0.15}NbO_3$ in one thermal cycle.

temperature range investigated. Otherwise, the grain capacitance, C_g, increases rapidly with temperature increasing. The dependence of grain capacitance on temperature obeys a Curie–Weiss type behavior. Curie's temperature is positioned at around 708 K at heating cycle. This temperature is very similar to reported previously, using an alternative approach where the bulk capacitance is extracted by the slope of the straight line determined by the variation of $-\mathrm{Im}(Z)$ as a function of $1/2\pi f$, at high frequency range (10^5–10^7 Hz).[15] However, Curie's temperature decreases at cooling cycle. In this work, Curie's temperature calculated from bulk capacitance values derived of theoretical adjust of the experimental data is positioned at around 650 K. Nevertheless, Curie's temperature calculated from capacitance values extracted at high frequency range, using an alternative approach[15] mentioned earlier, is positioned at 603 K. This temperature is similar to phase transition from orthorhombic to tetragonal (ferroelectric to ferroelectric) reported elsewhere.[15] It seems that the value of Curie's temperature derived at cooling cycle can be considered as an apparent one. The decreasing of Curie's temperature at cooling cycle is linked to the high level of superimposing of the temperature interval of the phase transitions[15] resulting to an underestimated value of Curie's temperature. The Curie–Weiss behavior exhibited by reciprocal grain capacitance, $1/C_g$ (Fig. 5), is characteristic of the bulk response of a normal ferroelectric material below 708 K, in accordance with following equation: $1/\epsilon=(T-T_C)/C$, where C is Curie's constant and T_C is the temperature of Curie, maximum ϵ. In the temperature range between 708 and 873 K, a small polarization degree can be observed probably correlated to existence of residual domains with structures of low symmetry. Above 873 K, C_g depends slightly on the temperature. At 708 K, no anomaly is identified on the grain boundary capacitance plot. This slight variation of the grain boundary capacitance as a function of temperature indicates a nonferroelectric state. A similar behavior is also observed from grain-boundary capacitance measurement during the cooling cycle, indicating a reasonable stability degree of grain boundary capacitance during the thermal cycle. This behavior provides further evidence of the presence of nonferroelectric phase at grain boundary, compatible with cubic symmetry.

The relaxation time (τ) can be determined by relation $\omega\tau=1$, where ω is angular frequency of relaxation ($\omega=2\pi f$). The relaxation time can be alternatively derived by the equation $\tau=RC$ where R is the resistance and C is the capacitance. The capacitance values can be extracted, if both parameters resistance and relaxation frequency are known, taking into account the previous equations.

The log τ_{gb} values of the first thermal cycle (heating and cooling cycles) were plotted as a function of reciprocal temperature $1/T$, as shown in Fig. 6. The experimental data are described by the expression Arrhenius type, given by the following equation:

$$\tau_{gb}=\tau_0 \exp(E_a/kT), \tag{4}$$

where τ_0 is the pre-exponential factor or characteristic relaxation time, derived at infinite temperature, and $E_{a\tau}$ is the activation energy for the relaxation, equal to 1.57 and 1.59 eV, for heating and cooling cycle, respectively. These values are similar those derived from conductivity plots, as can be seem in Fig. 4. The characteristic relaxation time of apparent polarization for the heating cycle is equal to $\tau_0=1.58\times10^{-12}$ s (i.e., $f_0=1.01\times10^{11}$ Hz) and for the cooling cycle τ_0 is equal to 1.25×10^{-12} s (i.e., $f_0=1.27\times10^{11}$ Hz). As can be observed, there is a slight difference between values for both characteristic relaxation times, which are compatible with thermal hysteresis. The relaxation characteristic time of the apparent polarization for the heating and cooling cycles shows that the relaxation process of grain boundary cannot be assigned to a dipole type relaxation.

IV. CONCLUSIONS

The grain boundary exhibits a electrical behavior compatible with poor semiconductor and linear dielectrical one. These properties imply in a nonferroelectric state. The nonferroelectric semiconductor character of the surface layer of the grain on the large temperature range and under heating and cooling cycle shows that the grain boundary region is not a region of acceptance of punctual-defect migration as

oxygen vacancy. Considering $Na_{0.85}Li_{0.15}NbO_3$ prepared in a stoichiometric manner and under air atmosphere, a definitive evidence for that it is not an ionic conductor was provided.

ACKNOWLEDGMENTS

This work was supported by the Brazilian research funding institutions FAPESP, CAPES and CNPq. The authors wish to acknowledge Companhia Brasileira de Metalurgia e Mineração-CBMM-Araxá-MG for supplying niobium complex salt used in this study.

[1] R. R. Zeyfang, R. M. Henson, and W. J. Maier, J. Appl. Phys. **48**, 3014 (1977).
[2] R. M. Henson, R. R. Zeyfang, and K. V. Kiehl, J. Am. Ceram. Soc. **60**, 15 (1977).
[3] H. D. Megaw, Ferroelectrics **7**, 87 (1974).
[4] I. Pozdnyakova, A. Navrotsky, L. Shilkina, and L. Reznitchenko, J. Am. Ceram. Soc. **85**, 379 (2002).
[5] S. Lanfredi, M. H. Lente, and J. A. Eiras, Appl. Phys. Lett. **80**, 2731 (2002).
[6] T. Nitta, J. Am. Ceram. Soc. **51**, 626 (1968).
[7] E. R. Leite, M. A. L. Nobre, E. Longo, and J. A. Varela, J. Am. Ceram. Soc. **80**, 2649 (1997).
[8] S. Lanfredi, L. Dessemond, and A. C. M. Rodrigues, J. Eur. Ceram. Soc. **20**, 983 (2000).
[9] Powder Diffraction File, Card No. 33-1270. Joint Committee on Powder Diffraction Standarts, Swarthmore, PA.
[10] M. Kleitz and J. H. Kennedy, in *Fast Ion Transport in Solids*, edited by P. Vashista, J. N. Mundy, and G. K. Shenoy (Elsevier, North Holland, 1979), pp. 185–188.
[11] M. A. L. Nobre and S. Lanfredi, J. Phys. Chem. Solids **62**, 1999 (2001).
[12] K. S. Cole and R. H. Cole, J. Chem. Phys. **9**, 341 (1941).
[13] A. R. James, S. Priya, K. Uchino, and K. Srinivas, J. Appl. Phys. **90**, 3504 (2001).
[14] S. Lanfredi, J. F. Carvalho, and A. C. Hernandes, J. Appl. Phys. **88**, 283 (2000).
[15] M. A. L. Nobre and S. Lanfredi, J. Phys.: Condens. Matter **12**, 7833 (2000).
[16] W. Bak, C. Kus, and W. S. Ptak, Ferroelectrics **115**, 105 (1991).